XXI IMEKO World Congress "Measurement in Research and Industry"
August 30 – September 4, 2015, Prague, Czech Republic

MAGNETOMETER BASED ON THE IMPEDANCE PHASE OF GMI SENSORS USING THE DMTD METHOD

D. M. Szwarcman [1], *E. Costa Silva* [1], *C. R. Hall Barbosa* [2], *E. Costa Monteiro* [2]

[1] Department of Electrical Engineering, PUC-Rio, Rio de Janeiro, Brazil, daniela.szw@gmail.com, edusilva@ele.puc-rio.br
[2] Postgraduate Program in Metrology, PUC-Rio, Rio de Janeiro, Brazil, hall@puc-rio.br, beth@puc-rio.br

Abstract – Giant Magnetoimpedance (GMI) sensors are a new family of magnetic sensing devices that show potential to detect ultra-weak magnetic fields. Recent studies demonstrated that phase-based GMI magnetometers can achieve very high sensitivities. This work aims at the development of an enhanced GMI magnetometer, based on a high resolution digital phase reading electronic circuit that makes use of the Dual Mixer Time Difference method, to read the impedance phase variations of GMI samples.

Keywords: impedance phase, giant magnetoimpedance, magnetic sensors, high resolution, DMTD

1. INTRODUCTION

Magnetic sensors are used in many applications, such as navigation systems, data storage devices, biomagnetic fields measurement, etc. Usually, magnetometers are rugged and reliable alternatives compared to other technologies [1-2].

The SQUID (Superconducting Quantum Interference Device) is the most adequate magnetometer for measuring very low intensity magnetic fields, as it is the most sensitive among all magnetic sensing devices. Nevertheless, this type of magnetometer has high costs of manufacturing and operation [1-2].

Magnetic transducers based on the GMI effect have been indicated in the literature as promising alternatives to SQUIDs, as they have good sensitivity and low cost for scale production [1-5].

The GMI effect is characterized by a large variation in the impedance of a magnetic conductor, when it is subjected to an external magnetic field [3-7]. Recent studies about GMI magnetometers have shown that the ones based on impedance phase readings are at least ten times more sensitive than those based on impedance magnitude characteristics [8-10].

The goal of this work is the development of a GMI magnetometer based on the phase characteristics of the sensor impedance using the Dual Mixer Time Difference (DMTD) method, aiming at achieving a low cost and accurate measuring system that can be employed in the measurement of low intensity magnetic fields.

This paper starts with a brief introduction to the GMI theory in section 2, followed by the results of the impedance characterization studies performed, in section 3. A detailed description of the phase detector circuit is given in section 4. Finally, the experimental results are presented in section 5 and the conclusions in section 6.

2. GIANT MAGNETOIMPEDANCE (GMI)

The impedance of a conductor usually depends on the material's current distribution. In high frequencies, the current tends to concentrate on the conductor surface. The skin depth in magnetic materials also depends on its geometry and magnetic permeability. Since the latter can vary with the applied magnetic field, changes in the impedance are expected for materials with high magnetic permeability, even for relatively low frequencies.

In GMI samples, an alternating current flowing through the material generates a transverse magnetic field, inducing its magnetization, and increasing the conductor permeability. As the skin depth depends on the magnetic permeability of the sample, the conductor impedance is modified according to the applied current and magnetic field [3-7].

Generally, the GMI curves, which represent the impedance variation as a function of external magnetic field, are symmetric with respect to this field. However, there are some factors that can cause asymmetry on these curves. This behavior is known as Asymmetric Giant Magnetoimpedance (AGMI) and can be induced by: DC current, AC magnetic field, exchange bias, etc [5, 11]. When properly adjusted, this asymmetry leads to large enhancements on the sample's sensitivity. In this work, the asymmetry was induced by DC currents. Fig. 1 shows a typical setup used to induce AGMI by means of DC currents on a ribbon shaped sample.

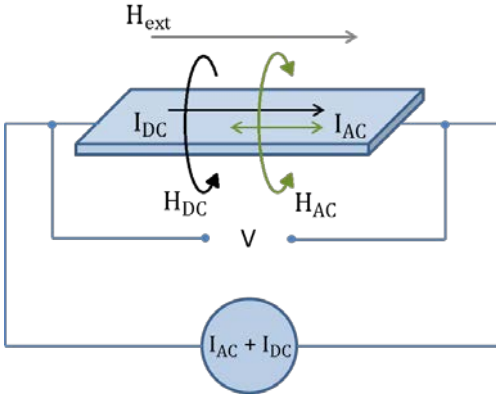

Fig. 1. Applied currents and fields on a GMI ribbon.

As shown in Fig. 1, the current must flow through the GMI sample in the same direction as the external magnetic field (H_{ext}). In this way, the current AC component (I_{AC}), generates an alternating circumferential magnetic field (H_{AC}) and its DC component generates a continuous circumferential magnetic field (H_{DC}). These fields promote a circumferential magnetization perpendicular to the direction of H_{ext}. In this case, the association of this magnetization with the magnetic helical anisotropy leads to asymmetric behavior in the GMI curves [5].

The GMI(%) is a figure of merit commonly used to evaluate variations of the impedance magnitude $|Z|$ of GMI samples, as a function of the magnetic field H [5]. It is defined as

$$\mathrm{GMI}(\%) = \left[\frac{|Z(H)|-|Z(H_{max})|}{|Z(H_{max})|}\right] \times 100\%, \qquad (1)$$

where H_{max} is a sufficiently large magnetic field, so that Z is saturated.

In order to exemplify the emergency of AGMI effect in a given GMI sample, Fig. 2 shows GMI(%) curves for different values of the DC current I_{dc}.

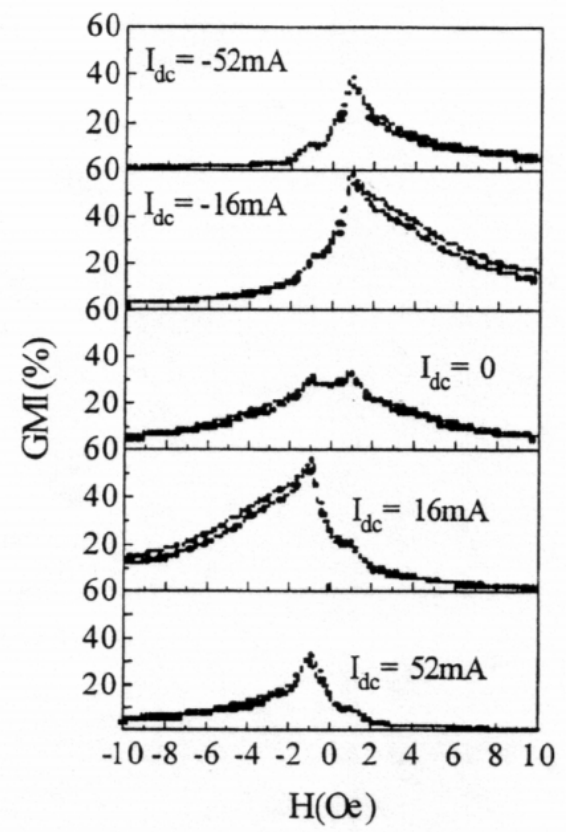

Fig. 2. AGMI effect induced by DC current [11].

The characteristics presented in Fig. 2 exhibit an almost symmetrical behavior in the absence of I_{dc} (center). On the other hand, comparing the GMI(%) curves for negative I_{dc} and for positive I_{dc}, it can be seen that the behavior is mirrored with respect to the vertical axis. Furthermore, the GMI(%) increases when I_{dc} goes from 0 mA to 16 mA, but decreases when I_{dc} is set to 52 mA. This means that there is a level of I_{dc} for which the GMI(%) is maximized which, in this case, lies between 0 mA and 52 mA.

3. IMPEDANCE CHARACTERIZATION

The sensitivity of GMI samples is typically affected by some parameters such as amplitude, frequency and DC level of the excitation current, dimensions (length, width, thickness) of the GMI samples, biasing magnetic field, among others. Therefore, the influence of these parameters under the GMI effect was experimentally investigated in order to ascertain which set of parameters generates optimum sensitivities [3-11].

The dependency on the excitation current DC level was studied between 0 mA and 100 mA as well as the dependency on its frequency, which was analyzed between 75 kHz and 30 MHz. It was also verified that variations of amplitude of the current AC component, around 15 mA, do not significantly affect the impedance behaviour of the analyzed samples. The measurements were performed with four different lengths: 1 cm, 3 cm, 5 cm and 15 cm.

The GMI sample used in this work has 3 cm length and was excited by a DC current of 80 mA and an AC current with 15 mA amplitude and 100 kHz frequency; because the phase sensitivity was maximized by this conditioning current. The resulting impedance magnitude and phase can be seen in Fig. 3.

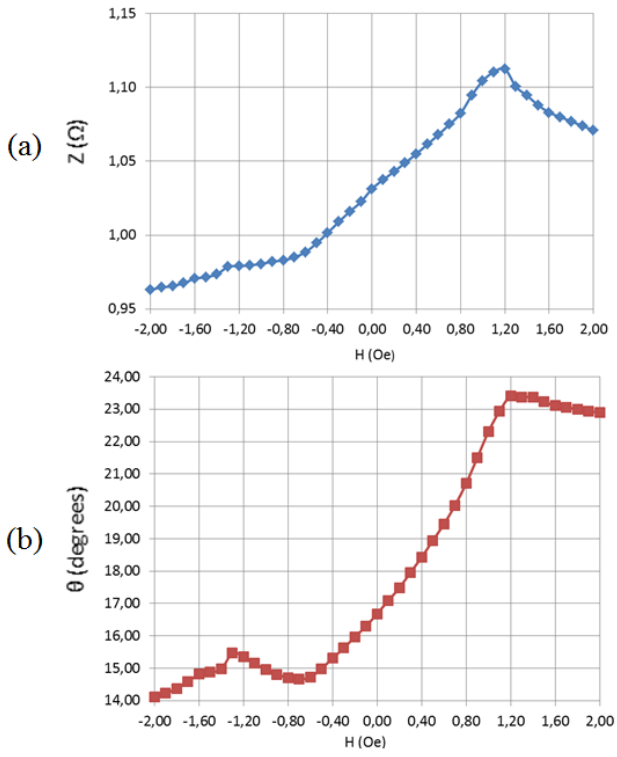

Fig. 3. GMI sample characterization: (a) impedance magnitude and (b) impedance phase.

Analyzing the experimental results presented in Fig. 3 one can concludes that the sensor has an average impedance phase sensitivity of 5.51° Oe^{-1}, in its almost-linear region (0 Oe to 1 Oe). Furthermore, as usual, it is intended to operate the sensor in its linear region. Then, aiming at maximizing the symmetric excursion inside this region, the sample should be biased at H_{bias} = 0.5 Oe.

4. PHASE DETECTOR CIRCUIT

To design a magnetometer based on phase characteristics of GMI samples, it is necessary to develop an electronic circuit capable of detecting the phase difference introduced by the sensor and associate it with the applied magnetic field.

The approach herein used for the phase detector combines analog circuits and a microcontroller. The sample is excited by a 100 kHz sinusoidal current together with a DC current; the voltage across the sample is then high-pass filtered, amplified and applied to a circuit comprised by a mixer, a low-pass filter and a comparator. The sample excitation signal is also applied to an all-pass filter, which introduces a 90º phase shift, and then it goes to an identical circuit set. Mixers are used to multiply sinusoidal signals with frequencies of 100 kHz and 99 kHz, so as the output is a signal with components in 1 kHz and 199 kHz. The high frequency component is cancelled by a low-pass filter and the phase comparison is done using the 1 kHz signals. Next, the sinusoidal signals are processed by comparators, configured as null detectors, and so converted to square waves with voltage levels compatible with the microcontroller inputs.

Finally, an internal timer measures the time difference correspondent to the phase shift between the 1 kHz input waves and calculates the corresponding phase in degrees. The phase shift is directly proportional to the magnetic field applied to the GMI sample. Fig. 4 shows the circuit's block diagram that will be analyzed in the next four subsections.

4.1. Signal Generation

Square wave oscillators and band-pass filters are used to generate the sinusoidal signals with frequencies of 100 kHz and 99 kHz that are going to be multiplied later. The band-pass filter has a narrow band around the fundamental frequency of the square waves. It is used to turn the square waves into sinusoidal waves and also to attenuate the power line interference (60 Hz) and other sources of electric interference. The resulting 100 kHz sinusoidal signal is applied to the sample (AC excitation) and it is also shifted by 90º (reference signal). The phase of this reference signal is not affected by the magnetic field, in contrast to the phase of the signal measured across the GMI sample, which changes according to the magnetic field.

The 90º phase shift was introduced to eliminate the need of a very fast response of the microcontroller: with quadrature signals, even for a small angle ϕ introduced by the sensor impedance, the phase shift between reference and sample signals will be large ($90^o + \phi >> \phi$). According to the characterization data, shown in Fig. 3, the phase angle introduced by the sample at H_{bias} is about 19º. Then, when the GMI sample is subjected to H_{bias} only, the phase difference between the two signals, can be obtained by subtracting 90º from 19º, leading to 71º.

4.2. Sample excitation circuit

Fig. 5 shows the sample excitation circuit and the applied currents: I_{DC} (80 mA) and I_{AC} (15 mA peak). The mosfet FDC6306P is configured as a DC current source, used to supply I_{DC} to the sample. The 200 Ω resistor was employed to set the amplitude of the AC current that flows through the GMI sample in 15 mA.

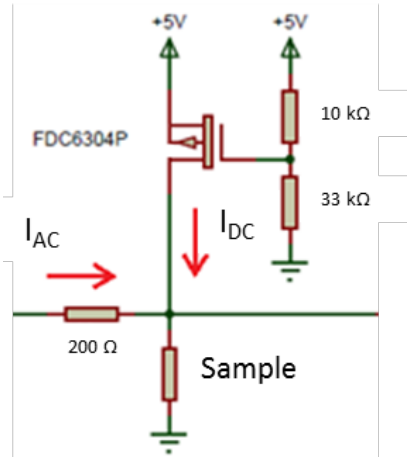

Fig. 5. GMI sample excitation circuit.

The resultant sample voltage is a sine wave of reduced amplitude (around 15 mV), due to its small impedance (about 1 Ω), added to a DC level (around 80 mV). Then, prior to be connected to the mixer input, this signal must be properly conditioned. A passive high-pass RC filter is needed to remove the DC level, so it can be amplified (100 times) by an instrumentation amplifier, without risking to violate the voltage limits of the mixer inputs.

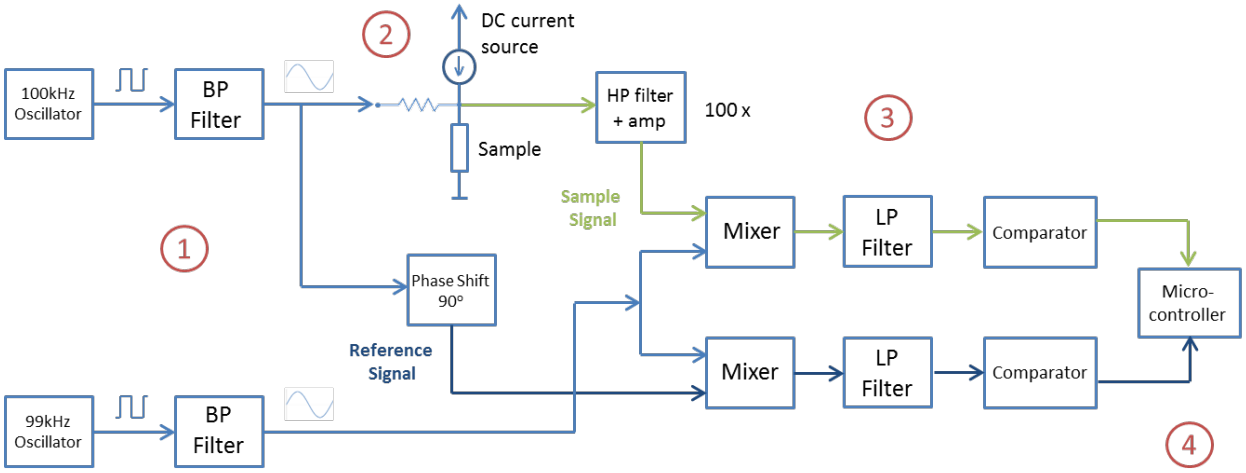

Fig. 4. Block diagram: 1 - Signal Generation, 2 - Sample excitation, 3 - Signal multiplication, 4 - Phase shift analysis.

4.3. Signal multiplication

In the DMTD method (Dual Mixer Time Difference) - Fig. 6 - two mixers are used to multiply a higher frequency (f_1) signal by another one with a slightly smaller frequency (f_2). This will generate a signal with two components: one in the sum frequency (f_1 + f_2) and one in the difference frequency (f_1 - f_2). This is explained by the basic trigonometric relation

$$cos(a) \times cos(b) = \frac{1}{2}[cos(a+b) + cos\,(a-b)], \quad (2)$$

so that

$$cos(2\pi f_1 t + \varphi) \times cos(2\pi f_2 t) = \frac{1}{2}[cos(2\pi(f_1+f_2)t + \varphi) + cos(2\pi(f_1-f_2)t + \varphi)]. \quad (3)$$

Therefore, since the angle φ is maintained after the multiplication process, it is possible to analyze the phase shift using a lower frequency signal (f_1 - f_2), which means measuring a larger time interval. This can improve the sensor resolution without the need of increasing the timer's clock frequency [12]. The outputs of the low-pass filters are connected to the inputs of the comparators, configured as null detectors, and the sinusoids become square waves with the same phase difference. Later, the time interval corresponding to the phase shift is measured.

In this work, the DMTD method was used to convert a phase difference between two 100 kHz signals into the same phase difference between 1 kHz signals.

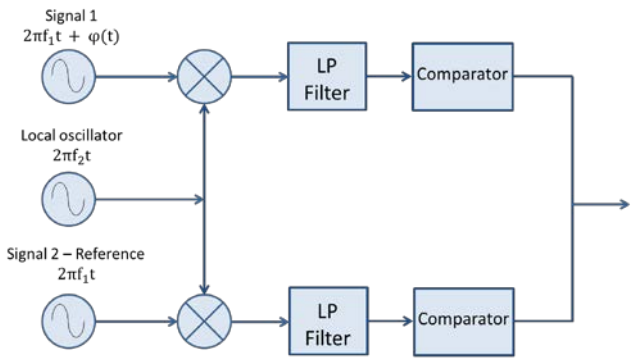

Fig. 6. DMTD - scheme.

4.4. Phase shift analysis

In the proposed circuit, the role of the microcontroller is to measure the phase difference between the reference and the sample signals, by evaluating the time interval between them - as shown in Fig. 7.

A timer, internal to the microcontroller, counts from 0 to FFFF (hexadecimal) with a 2 MHz clock, uninterruptedly. When a positive signal transition (logical 0 to logical 1) occurs at specific input ports of the microcontroller, it saves on a register the timer count, at that moment.

The positive transition of the reference signal saves the count value t_1 while the positive transition of the sample signal saves the count value t_2. Then, the microcontroller calculates the time difference $|t_2 - t_1|$ and the corresponding angle in degrees. The results are show on a LCD display.

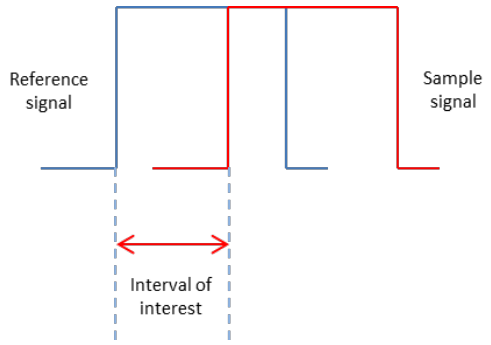

Fig. 7. Time interval corresponding to the phase difference.

It is important to notice that, for a clock frequency of 2 MHz, the minimal time that can be measured is 500 ns. This value corresponds to a 0.18º angle for a 1 kHz signal. With an average impedance phase sensitivity of 5.51º Oe^{-1}, a variation of 0.18º corresponds to a variation of 0.033 Oe. A straightforward way to improve the digital resolution is to increase the clock frequency. For instance, if it is ten times higher, the resolution will improve by a factor of ten. Besides that, it is possible to adjust the local oscillator to provide a frequency closer to 100 kHz, making the difference frequency lower than 1 kHz. For example, if the local oscillator has a frequency of 99.9 kHz, the difference frequency will be 100 Hz and then the microcontroller will measure time intervals of 100 Hz signals.

5. EXPERIMENTAL RESULTS

According to Fig. 3, the impedance magnitude varies around 1 Ω. Based on that, aiming at verifying the general operation of the electronic circuit, it was initially tested with a 1 Ω resistor in the place of the GMI sample. After verifying that the circuit was working properly, the resistor was replaced by the GMI and the final tests were performed.

Fig. 8 shows the voltage signal measured between the terminals of the 1 Ω resistor. Both the AC amplitude and the DC level agree with the expected values. However, the presence of higher frequency noise was observed. The unwanted frequencies lie in the range between 700 kHz and 1.3 MHz, according to the spectral analysis shown in Fig. 8 (b). To reduce this noise, the circuit can be shielded.

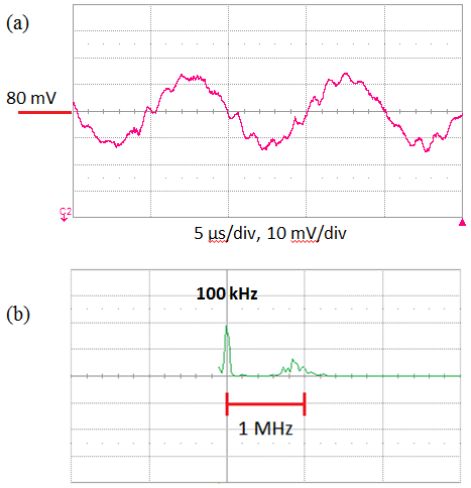

Fig. 8. (a) Voltage across the 1 Ω resistor and (b) signal spectrum.

The reference signal is shifted by 90° and the sample signal has a null phase shift, since the GMI sample was substituted by a 1 Ω resistor. Following that, those signals are multiplied by two different mixers. Fig. 9 shows the mixer output, its spectrum and the high frequency attenuation. The results are similar for both mixers.

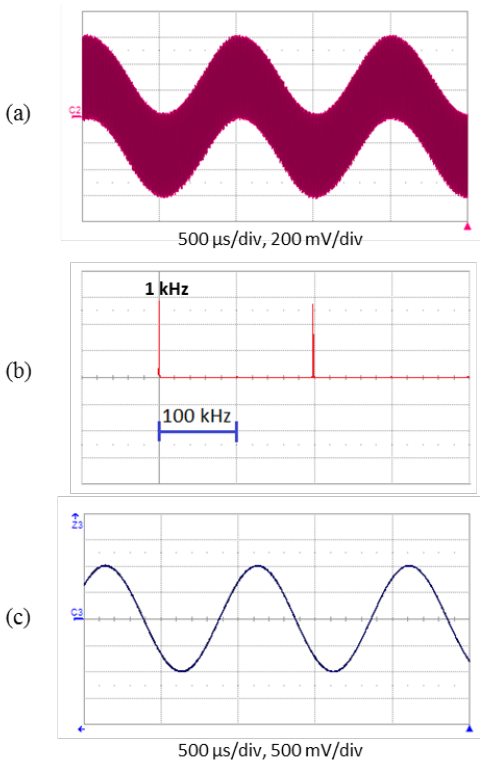

Fig. 9. (a) Mixer's output, (b) its spectrum and (c) the result after filtering the 199 kHz frequency.

Now, both the reference signal and the sample signal have frequencies of 1 kHz, as it can be seen in Fig. 10. The phase difference between them, measured with an oscilloscope, is 104.3°. This value is higher than the expected 90°, because the stage comprising the high-pass filter and the instrumentation amplifier, shown in Fig. 4, introduce an additional phase shift. Nevertheless, it will not affect the circuit's performance, since this phase shift is constant and does not change with the external magnetic field.

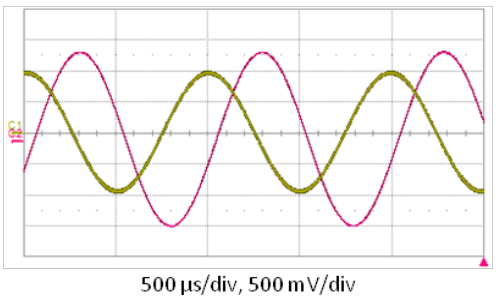

Fig. 10. Reference signal (smaller) and sample signal (larger) after multiplication and high frequency attenuation.

Finally, the comparators convert these signals into square waves, as shown in Fig. 11.

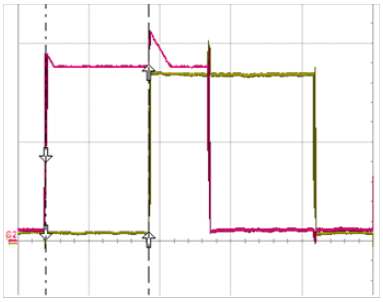

Fig. 11. Comparators' output.

Thus, the microcontroller can measure the time interval between the positive transitions of the two signals and calculate the corresponding phase difference. The result, shown at the LCD display, has indicated a phase difference of 104.04°. This value is close enough to the one measured by the oscilloscope and can be considered satisfactory.

Finally, the 1 Ω resistor was substituted by the ribbon-shaped GMI sample. The magnetic field was varied between 0 Oe and 1 Oe, where the impedance phase shows an almost linear behavior (Fig. 3). The mean sensitivity obtained with the magnetometer was 3.6° Oe^{-1}, which is less than the 5.51° Oe^{-1} obtained in the experimental characterization presented in section 3.

The difference between the sensitivities of the isolated sample and of the complete magnetometer can be explained by the inductance of the wires used to connect the ribbon to the phase detector circuit. This inductance is added in series with the sensor's impedance, but it does not change with the magnetic field, thus reducing the overall sensitivity.

6. CONCLUSION

The results obtained show that the developed phase reading technique has potential to enhance the performance of phase-based GMI magnetometers, aiming at the measurement of weak magnetic fields.

Even with satisfactory results, the analog part of the circuit can be improved by using shielding techniques to reduce the high frequency noise. The use of a microcontroller allows the storage of data, for posterior analysis of results.

Besides that, the digital resolution can be improved by increasing the clock frequency or by decreasing the frequency of the signals connected to the microcontroller inputs. In future works, the connection of the GMI ribbon to the circuit will be optimized, to reduce the effect of spurious impedances. Also, the overall measuring system uncertainty will be estimated.

ACKNOWLEDGMENTS

We thank the Brazilian funding agencies FINEP, CAPES, CNPq and FAPERJ, for their financial support.

REFERENCES

[1] A. E. Mahdi, L. Panina and D. Mapps, "Some new horizons in magnetic sensing: high-Tc SQUIDs, GMR and GMI materials", *Sensors and Actuators A*, vol. 105, nº. 3, pp. 271–285, 2003.

[2] J. Lenz and A. S. Edelstein, "Magnetic Sensors and Their Applications", *IEEE Sensors Journal*, vol. 6, nº. 3, pp. 631–649, 2006.

[3] C. Tannous and J. Gieraltowski, "Giant magneto-impedance and its applications", *J. Mat. Sci.*, vol. 15, nº. 3, pp. 125–133, 2004.

[4] H. Hauser, L. Kraus and P. Ripka, "Giant magnetoimpedance sensors", *IEEE Instrum. Meas. Mag.*, vol. 4, nº. 2, pp. 28–32, 2001.

[5] M-H Phan and H-X Peng, "Giant magnetoimpedance materials: fundamentals and applications", *Prog. Mater. Sci.*, vol. 53, nº. 2, pp. 323–420, 2008.

[6] V. Knobel and K. R. Pirota, "Giant magnetoimpedance concepts and recent progress", *J. Magn. Magn. Mater.*, vol. 242, pp. 33–40, 2002.

[7] L. Kraus, "GMI modeling and material optimization", *Sens. Actuators A*, vol. 106, pp. 187–194, 2003.

[8] E. Costa Silva, L. A. P. Gusmão, C. R. Hall Barbosa, E. Costa Monteiro and F. L. A. Machado, "High sensitivity giant magnetoimpedance (GMI) magnetic transducer: magnitude versus phase sensing", *Meas. Sci. Technol.*, vol. 22, nº. 3, pp. 035204, 2011.

[9] E. Costa Silva, L. A. P. Gusmão, C. R. Hall Barbosa, and E. Costa Monteiro, "Electronic approach for enhancing impedance phase sensitivity of GMI magnetic sensors", *Electronics Letters*, vol. 49, pp. 396–397, 2013.

[10] E. Costa Silva, L. A. P. Gusmão, C. R. Hall Barbosa and E. Costa Monteiro. "An enhanced electronic topology aimed at improving the phase sensitivity of GMI sensors", *Meas. Sci. Technol.*, vol. 25, nº. 11, pp. 115010, 2014.

[11] F. L. A. Machado, A. R. Rodrigues, A. A. Puça, A. E. P. de Araújo, "Highly Asymmetric Giant Magnetoimpedance", *Mater. Sci. Forum*, vol. 302-303, nº. 202–208, 1999.

[12] F. Nakagawa, M. Imae, Y. Hanado and M. Aida, "Development of Multichannel Dual-Mixer Time Difference System to Generate UTC (NICT)", *IEEE Trans. Instrum. Meas.*, vol. 54, nº. 2, pp. 829–832, 2005.